SCIENCE AND TECHNOLOGY ORGANIZATION
CENTRE FOR MARITIME RESEARCH AND EXPERIMENTATION

Reprint Series CMRE-PR-2019-087

Long-term vessel kinematics prediction exploiting mean-reverting processes

Leonardo M. Millefiori, Paolo Braca, Karna Bryan, Peter Willett

June 2019

Originally published in:

19th International Conference on Information Fusion, 5-8 July 2016, Heidelberg, Germany, pp. 232-239

About CMRE

The Centre for Maritime Research and Experimentation (CMRE) is a world-class NATO scientific research and experimentation facility located in La Spezia, Italy.

The CMRE was established by the North Atlantic Council on 1 July 2012 as part of the NATO Science & Technology Organization. The CMRE and its predecessors have served NATO for over 50 years as the SACLANT Anti-Submarine Warfare Centre, SACLANT Undersea Research Centre, NATO Undersea Research Centre (NURC) and now as part of the Science & Technology Organization.

CMRE conducts state-of-the-art scientific research and experimentation ranging from concept development to prototype demonstration in an operational environment and has produced leaders in ocean science, modelling and simulation, acoustics and other disciplines, as well as producing critical results and understanding that have been built into the operational concepts of NATO and the nations.

CMRE conducts hands-on scientific and engineering research for the direct benefit of its NATO Customers. It operates two research vessels that enable science and technology solutions to be explored and exploited at sea. The largest of these vessels, the NRV Alliance, is a global class vessel that is acoustically extremely quiet.

CMRE is a leading example of enabling nations to work more effectively and efficiently together by prioritizing national needs, focusing on research and technology challenges, both in and out of the maritime environment, through the collective Power of its world-class scientists, engineers, and specialized laboratories in collaboration with the many partners in and out of the scientific domain.

19th International Conference on Information Fusion
Heidelberg, Germany - July 5-8, 2016

CMRE-PR-2019-087

Long-Term Vessel Kinematics Prediction Exploiting Mean-Reverting Processes

Leonardo M. Millefiori*, Paolo Braca*, Karna Bryan*, and Peter Willett†
*NATO STO-CMRE, La Spezia, Italy, Email: {leonardo.millefiori,paolo.braca,karna.bryan}@cmre.nato.int
†University of Connecticut, Storrs CT, Email: willett@engr.uconn.edu

***Abstract*—Long-term target state estimation of non-maneuvering targets, such as vessels under way in open sea, is crucial for maritime security.**

The dynamics of non-maneuvering targets is traditionally modeled with a white noise random process on the velocity, which is assumed to be nearly-constant. We show that this model might be an implausible hypothesis for a significant portion of maritime ship traffic, as vessels under way tend to adjust their speed continuously around a desired value. Additionally, vessels will naturally seek to optimize fuel consumption.

We developed a method to predict long-term target states based on mean-reverting stochastic processes. Specifically, we use the Ornstein-Uhlenbeck (OU) process, leading to a revised target state equation and to a completely different time scaling law for the related uncertainty, which in the long term is shown to be orders of magnitude lower than nearly-constant velocity assumption.

The proper modeling provides some improvement in accuracy; but the real benefit is improved track-stitching when there are lengthy gaps in observability. In support of the proposed model, we propose a large-scale analysis of a significant portion of the real-world maritime traffic in the Mediterranean Sea.

I. Introduction

Ship traffic monitoring is a foundation for many maritime security domains, and modern monitoring system specifications and requirements reflect the need for an extended and continuous ability to track vessels beyond territorial waters and over several sensor coverage areas. However, vessels in open seas are seldom *continuously* observed by monitoring sensors and even the data coming from self-reporting systems is often highly intermittent.

The problem of *long-term* vessel state estimate and prediction is therefore crucial for safety at sea. Unfortunately, this issue has been overlooked in the target tracking literature, and only few works partially address the problem, e.g. [1]–[3], while most of the literature is focused on maneuvering target models, e.g. [4]–[6].

On the other hand, real-world self-reported data (i.e., largely Automatic Identification System (AIS) [7], [8]) shows that a significant portion of the vessels in open seas maneuver very seldom. In the literature, non-maneuvering target dynamics are modeled with a velocity that is perturbed by a white noise process. This model is often referred as Nearly Constant Velocity (NCV) [5], [9] and has been successfully used in several target tracking applications, such as radar [10] and sonar [11], where the prediction step always refers to the very near future, generally one sensor time-scan ahead. The NCV model is adopted also in [1] for anomaly detection and motion prediction.

We propose [12]–[14] a method for the long-term prediction of target states based on the Ornstein-Uhlenbeck (OU) stochastic process, which leads to a revised target state equation and to a completely different time scaling law for the related uncertainty. This formulation reduces by an order of magnitude the uncertainty region of the predicted position with respect to the models available in the literature.

This aspect is crucial for several applications. To mention one, in Search and Rescue (SaR) operations, a smaller uncertainty region implies a smaller search region, which can significantly improve the probability of success for search cases. For instance, let us consider a vessel having an accident in a region with intermittent AIS coverage (e.g. open sea); the position of the accident is consequently unknown. Not having any information other than its last observed position and the time of accident (e.g. time of SOS message), the only possibility is to hypothesize that the ship had been moving from the last observation to the position of the accident in a straight line. It is important to notice that this assumption has to be made whether the traditional or the proposed approach is taken. The important difference is that using the proposed method, the search area (the uncertainty region) would increase linearly (instead of quadratically) in proportion to the time from last report, for a given level of confidence.

The OU model can be seen as a modified Wiener process with a tendency for the walk to return to a central location, with a greater attraction when the process is further away from the center. It is popular in various and heterogeneous scientific fields, spanning from physics to finance and biology, but it is much less popular within the tracking community [15].

To the best of the authors' knowledge, only few works consider the OU model for the target dynamics, and none of them use it for long-term target state prediction. In the tracking literature, the OU model has been discussed mostly notably by Coraluppi and Carthel in [16]–[19], where the stability of the OU, and the so-called Mixed Ornstein-Uhlenbeck (MOU) processes are studied.

However all of these works, including [15], deal with *zero-mean-reverting* processes, i.e. the typical velocities are null, the aim not being the long-term target state prediction, but rather the short-term characterization of the target dynamics. Indeed, in [16] the authors are more interested in the boundedness of the target components, and for this reason the MOU is

978-0-9964527-4-8©2016 ISIF

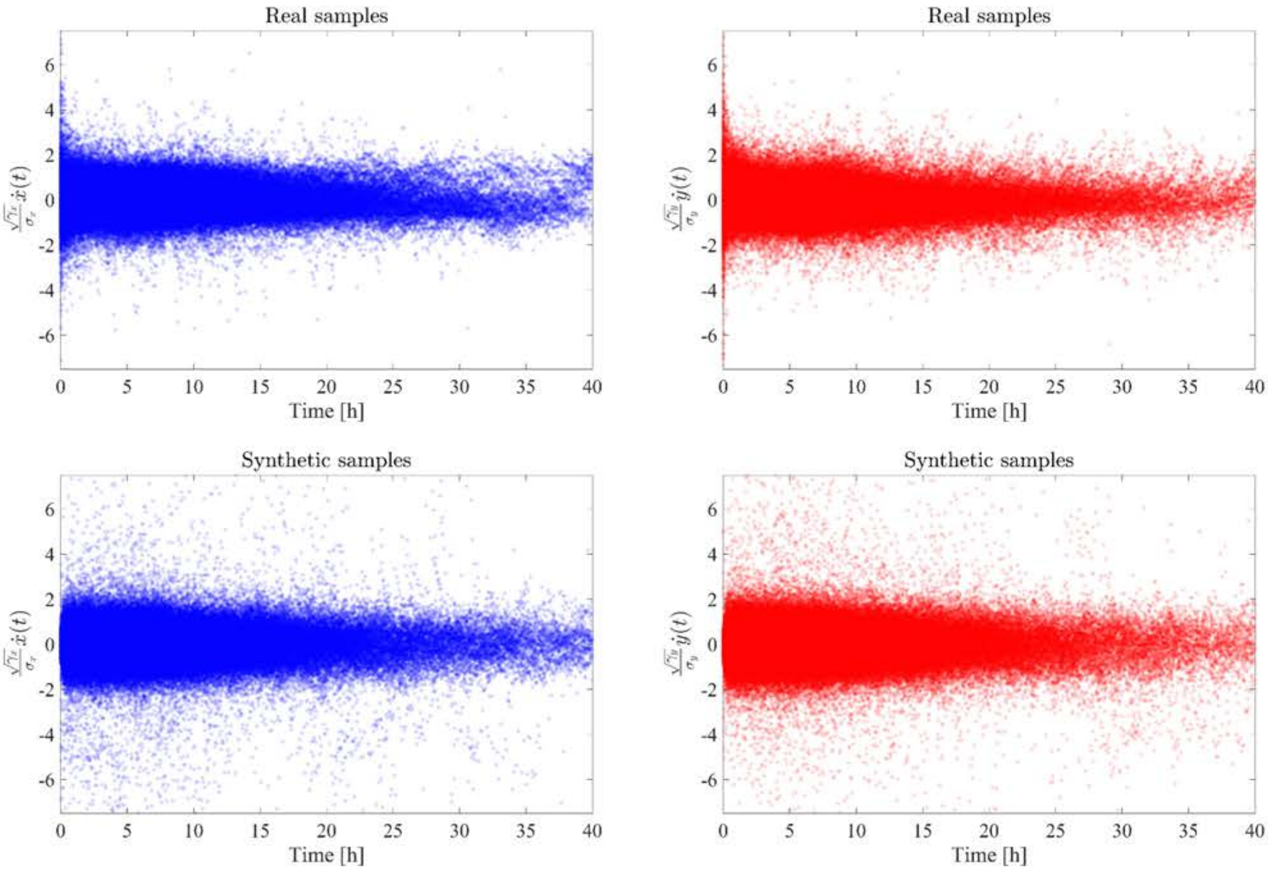

Fig. 1. Normalized samples of the x (left) and y component of the target velocity versus time. Scatter plots in the top row are generated from real-world speed samples of ships under way in the Mediterranean Sea, while those in the second row show synthetic OU samples. The real-world and synthetic data sets have the same cardinality.

a zero-mean-reverting process for both position and velocity.

In contrast to [15]–[19], in this paper we focus on the long-term prediction of non-maneuvering vessels, such as those under way in the open sea. We show that that the NCV is implausible for a significant portion of maritime ship traffic, as vessels under way tend to continuously adjust their speeds around a desired operating point. This is intuitively illustrated by Fig. 1, where the scatter plots in the first row come from —conveniently scaled— real-world ship speed samples, while those in the second row are generated from a synthetic data set of OU samples, for the x (left) and y (right) components of the target velocity.

Supported by real-world vessel traffic data, we show that mean-reverting processes can be used to model non-maneuvering vessel movement. Specifically, we provide evidence that the vessel velocity is well-described by an OU stochastic process, and consequently the vessel position by an Integrated Ornstein-Uhlenbeck (IOU) process. As a consequence, after an initial transient, the vessel position is mathematically equivalent to Brownian particle motion. It is also shown that the popular NCV model that is commonly adopted in the target tracking literature is not well-suited for the characterization of the uncertainty of the long-term target state prediction. While it is sufficiently accurate for short-term predictions (typically the case for traditional target tracking applications) the NCV model can overestimate the actual uncertainty of long-term predictions, even to orders of magnitude.

Our results are supported by an extensive analysis of a data set of real-world vessel trajectories. For each of them, the OU and NCV process parameters are estimated using a Maximum Likelihood (ML) procedure. The OU and NCV models are then compared in terms of capability to represent statistically the prediction error variance against the prediction horizon time. Specifically, the experimental normalized prediction variance curve, averaged among all the available trajectories, is compared against the theoretical normalized variance curve of the OU and NCV models. Based on this validation criterion, we show that the OU process better models the behavior of a significant portion of real-world vessels than the NCV. The proposed estimator, based on the OU process, is then demonstrated to be suitable for long-term prediction in practical applications. Moreover, the prediction uncertainty equation has a closed-form expression, provided by the OU process characterization, which is very useful in real-world use cases.

The paper is organized as follows. In Section II we formalize the problem in terms of a stochastic differential equation (SDE) for the target motion and introduce the OU and NCV models. Section III is devoted to the model parameter estimation procedure, while in Section IV we formalize the model validation criterion. Finally, experimental results are reported in Section V. This paper is a focused version of [14].

II. Vessel dynamic models

Let us indicate the target state at the time $t \in \mathbb{R}_0^+$ with

$$\boldsymbol{s}(t) \overset{def}{=} [x(t),\, y(t),\, \dot{x}(t),\, \dot{y}(t)]^T, \tag{1}$$

where the two coordinates $x(t)$ and $y(t)$, and the corresponding velocities $\dot{x}(t)$ and $\dot{y}(t)$, in a two-dimensional Cartesian (x, y) reference system are also denoted by

$$\boldsymbol{x}(t) \overset{def}{=} [x(t),\, y(t)]^T \tag{2}$$

$$\dot{\boldsymbol{x}}(t) \overset{def}{=} [\dot{x}(t),\, \dot{y}(t)]^T. \tag{3}$$

The choice to define the target state in the Cartesian coordinates is standard in the target tracking literature, e.g. see [9]. In this formulation of the problem (x, y) can be either the Universal Transverse Mercator (UTM) coordinate system, or the rotated coordinate along the target trajectory, as usually assumed in the knowledge-based tracking, e.g. see [20]–[22].

Let the target dynamics be a set of linear SDE [5]:

$$\mathrm{d}\boldsymbol{s}(t) = \boldsymbol{A}\boldsymbol{s}(t)\,\mathrm{d}t + \boldsymbol{G}\boldsymbol{u}(t)\,\mathrm{d}t + \boldsymbol{B}\,\mathrm{d}\boldsymbol{w}(t), \tag{4}$$

where $\boldsymbol{A}$, $\boldsymbol{B}$ and $\boldsymbol{G}$ are constant matrices, $\boldsymbol{u}(t)$ is a deterministic function, and $\boldsymbol{w}(t)$ is a standard bi-dimensional Wiener process. The SDE can be solved by the use of Itô calculus [23].

Given the state of a target $\boldsymbol{s}(t_0)$ observed at the time t_0, we aim to predict its state at the time t. This prediction can be carried out with an optimal Bayesian estimator:

$$\begin{aligned} \boldsymbol{s}(t|t_0) &\overset{def}{=} [x(t|t_0), y(t|t_0), \dot{x}(t|t_0), \dot{y}(t|t_0)]^T \\ &= \mathrm{E}\left[\boldsymbol{s}(t)\,|\boldsymbol{s}(t_0)\right], \end{aligned} \tag{5}$$

where $\mathrm{E}[\cdot]$ indicates the expectation operator. As opposed to conventional tracking applications, we are interested in exploring the properties of $\boldsymbol{s}(t|t_0)$ when $t - t_0$ is not comparable to the refresh rate of the sensor that issues the measurements, being instead orders of magnitude above it. The estimator (5) is highly dependent on the underlying motion model described by the SDE (4). We will focus only on the case of non-maneuvering target, as for a vessel while under way.

Differently from the tracking literature, where the target state observation is typically affected by noise, we shall assume to observe directly the target positional state. This assumption is not binding, provided that a negligible measurement noise is even plausible with respect to the real-world data set presented in Section V and therein exploited for the prediction error variance analysis, because the vessel positions broadcast by AIS transmitters have the same accuracy as the Global Positioning System (GPS), and the measurement noise would be therefore negligible, especially if compared to the size of commercial ships.

One of the most popular target motion models, commonly adopted in the scientific target tracking literature, is the NCV model [5], where (4) has the form

$$\mathrm{d}\boldsymbol{s}(t) = \boldsymbol{A}\boldsymbol{s}(t)\,\mathrm{d}t + \boldsymbol{B}\,\mathrm{d}\boldsymbol{w}(t), \tag{6}$$

with

$$\boldsymbol{A} = \begin{bmatrix} \mathbf{0} & \boldsymbol{I} \\ \mathbf{0} & \mathbf{0} \end{bmatrix}, \quad \boldsymbol{B} = \begin{bmatrix} \mathbf{0} \\ \boldsymbol{C} \end{bmatrix}, \tag{7}$$

being $\boldsymbol{I}$ the bi-dimensional identity matrix, $\mathbf{0}$ the bi-dimensional null matrix and $\boldsymbol{C}$ a generic bi-dimensional matrix. In practice, the equation for the target dynamics relies on the fact that, for non-maneuvering vessels $\ddot{\boldsymbol{x}}(t) \approx [0, 0]^T$, i.e. there is a "small" effect on $\dot{\boldsymbol{x}}(t)$ that accounts for unpredictable modeling errors [5].

For the OU model the SDE has a slightly different form, with an additional term that accounts for the mean-reverting tendency of the velocity:

$$\mathrm{d}\boldsymbol{s}(t) = \boldsymbol{A}\,\boldsymbol{s}(t)\,\mathrm{d}t + \boldsymbol{G}\,\boldsymbol{v}\,\mathrm{d}t + \boldsymbol{B}\;\mathrm{d}\boldsymbol{w}(t), \tag{8}$$

where $\boldsymbol{v} = [v_x, v_y]^T$, and $\boldsymbol{w}(t)$ is a standard bi-dimensional Wiener process. The matrices $\boldsymbol{A}$, $\boldsymbol{B}$ and $\boldsymbol{G}$ are defined as:

$$\boldsymbol{A} = \begin{bmatrix} \mathbf{0} & \boldsymbol{I} \\ \mathbf{0} & -\boldsymbol{\Theta} \end{bmatrix}, \quad \boldsymbol{B} = \begin{bmatrix} \mathbf{0} \\ \boldsymbol{C} \end{bmatrix}, \quad \boldsymbol{G} = \begin{bmatrix} \mathbf{0} \\ \boldsymbol{\Theta} \end{bmatrix}, \tag{9}$$

being $\boldsymbol{\Theta}$ and $\boldsymbol{C}$ generic bi-dimensional matrices. Equation (8) has the form of a Langevin dynamic [24] and can be solved in closed form by using Itô calculus [23], [25]. The $\dot{\boldsymbol{x}}(t)$ process is said to be of the Ornstein-Uhlenbeck (OU) type [26], [27] and correspondingly, we say that $\boldsymbol{x}(t)$ is an Integrated Ornstein-Uhlenbeck (IOU) process [27]. The parameters v_x and v_y in $\boldsymbol{v}$ play a key role in the proposed model because they represent the *typical* velocities along x and y, respectively, of the vessel on the trajectory under consideration. Roughly speaking, the velocity of the process tends to drift over time towards its long-term mean; and the mean-reversion tendency is stronger when the velocity is further away from that long-term mean.

The diagonal terms of $\boldsymbol{\Theta}$ represent the mean reversion effect along the x and y components, respectively, while the off-diagonal elements measure the coupling effect between them. Assuming that $\boldsymbol{\Theta}$ is diagonalizable and has positive eigenvalues, an affine transformation can be found that projects the matrix $\boldsymbol{\Theta}$ onto another space, i.e., $\boldsymbol{\Theta} = \boldsymbol{R}\boldsymbol{\Gamma}\boldsymbol{R}^{-1}$, where $\boldsymbol{\Gamma}$ is diagonal. This idea is expanded further in [14], where we also provide the general solution to the coupled problem. However, for the sake of brevity, in this work we assume that $\boldsymbol{\Theta} = \boldsymbol{\Gamma} = \mathrm{diag}(\boldsymbol{\gamma})$ is diagonal and $\boldsymbol{\gamma} = [\gamma_x, \gamma_y]^T$.

A. Prediction procedure

The solution of the SDE provides for the target state prediction $\boldsymbol{s}(t\,|t_0)$ and the related variance, which we will take as a measure of the prediction uncertainty. In this section we will describe the prediction procedure in the two cases that the OU and NCV models are assumed for the target velocity.

1) Nearly Constant Velocity (NCV) model: Assuming the NCV model for the velocity of the target, we have that the optimal prediction, given the initial target state $\boldsymbol{s}(t_0)$, is the following [9]

$$\boldsymbol{s}(t|t_0) = \boldsymbol{F}(t-t_0)\boldsymbol{s}(t_0), \tag{10}$$

where $\boldsymbol{F}(t)$ is often referred to as the state transition matrix and is given by

$$\boldsymbol{F}(t) = \begin{bmatrix} \boldsymbol{I} & t\,\boldsymbol{I} \\ \boldsymbol{0} & \boldsymbol{I} \end{bmatrix}. \tag{11}$$

According to (10), the covariance matrix of the estimator is provided by Itô calculus and is given by

$$\mathrm{Cov}\left[\boldsymbol{s}(t)\,|\boldsymbol{s}(t_0)\right] = \begin{bmatrix} \frac{(t-t_0)^3}{3} & \frac{(t-t_0)^2}{2} \\ \frac{(t-t_0)^2}{2} & t-t_0 \end{bmatrix} \otimes \boldsymbol{C}\boldsymbol{C}^T, \tag{12}$$

where

$$\boldsymbol{C}\boldsymbol{C}^T = \begin{bmatrix} \sigma_x^2 & \sigma_{xy} \\ \sigma_{xy} & \sigma_y^2 \end{bmatrix}.$$

2) Ornstein-Uhlenbeck (OU) model: Let us consider the case in which the velocity of the target follows the OU model. We have that the optimal prediction, given the initial target state, is provided by the first moment of the SDE solution [25], [27] and, for the velocity, we have

$$\dot{\boldsymbol{x}}(t|t_0) = \boldsymbol{v} + \begin{bmatrix} \mathrm{e}^{-\gamma_x(t-t_0)} & 0 \\ 0 & \mathrm{e}^{-\gamma_y(t-t_0)} \end{bmatrix} (\dot{\boldsymbol{x}}(t_0) - \boldsymbol{v}). \tag{13}$$

Proceeding similarly for the target position, which is an IOU process, the following expression can be derived

$$\boldsymbol{x}(t|t_0) = \boldsymbol{x}(t_0) + (t-t_0)\,\boldsymbol{v} + \begin{bmatrix} \frac{1-\mathrm{e}^{-\gamma_x(t-t_0)}}{\gamma_x} & 0 \\ 0 & \frac{1-\mathrm{e}^{-\gamma_y(t-t_0)}}{\gamma_y} \end{bmatrix} (\dot{\boldsymbol{x}}(t_0) - \boldsymbol{v}). \tag{14}$$

The optimal prediction can be rearranged in the matrix form

$$\boldsymbol{s}(t|t_0) = \boldsymbol{\Phi}(t-t_0,\boldsymbol{\gamma})\,\boldsymbol{s}(t_0) + \boldsymbol{\Psi}(t-t_0,\boldsymbol{\gamma})\,\boldsymbol{v}, \tag{15}$$

where $\boldsymbol{\Phi}(t,\boldsymbol{\gamma})$ is the analog of the state transition matrix and $\boldsymbol{\Psi}(t,\boldsymbol{\gamma})\,\boldsymbol{v}$ is often called the control input function, defined as

$$\boldsymbol{\Phi}(t,\boldsymbol{\gamma}) \stackrel{def}{=} \mathrm{e}^{\tilde{\boldsymbol{A}}t} = \begin{bmatrix} \boldsymbol{I} & \left(\boldsymbol{I} - \mathrm{e}^{-\boldsymbol{\Gamma}t}\right)\boldsymbol{\Gamma}^{-1} \\ \boldsymbol{0} & \mathrm{e}^{-\boldsymbol{\Gamma}t} \end{bmatrix}, \tag{16}$$

and

$$\boldsymbol{\Psi}(t,\boldsymbol{\gamma}) = \begin{bmatrix} t\,\boldsymbol{I} - \left(\boldsymbol{I} - \mathrm{e}^{-\boldsymbol{\Gamma}t}\right)\boldsymbol{\Gamma}^{-1} \\ \boldsymbol{I} - \mathrm{e}^{-\boldsymbol{\Gamma}t} \end{bmatrix}. \tag{17}$$

We provide the full form of the estimator covariance matrix in [14]. For the sake of brevity, we report here only the variance terms:

$$\mathrm{E}\left[(x(t|t_0) - x(t))^2|\,\boldsymbol{s}(t_0)\right] = \frac{\sigma_x^2}{\gamma_x^3} f(\gamma_x\,(t-t_0)) \tag{18}$$

$$\mathrm{E}\left[(y(t|t_0) - y(t))^2|\,\boldsymbol{s}(t_0)\right] = \frac{\sigma_y^2}{\gamma_y^3} f(\gamma_y\,(t-t_0)) \tag{19}$$

$$\mathrm{E}\left[(\dot{x}(t|t_0) - \dot{x}(t))^2|\,\boldsymbol{s}(t_0)\right] = \frac{\sigma_x^2}{\gamma_x} g(\gamma_x\,(t-t_0)) \tag{20}$$

$$\mathrm{E}\left[(\dot{y}(t|t_0) - \dot{y}(t))^2|\,\boldsymbol{s}(t_0)\right] = \frac{\sigma_y^2}{\gamma_y} g(\gamma_y\,(t-t_0)) \tag{21}$$

where $f(t)$ and $g(t)$ are the prediction position and velocity error *normalized* variance, defined as

$$f(t) \stackrel{def}{=} \frac{1}{2}\left(2t + 4\mathrm{e}^{-t} - \mathrm{e}^{-2t} - 3\right) \tag{22}$$

$$g(t) \stackrel{def}{=} \frac{1}{2}\left(1 - \mathrm{e}^{-2t}\right), \tag{23}$$

where σ_x^2 and σ_y^2 are the diagonal elements of $\boldsymbol{C}\boldsymbol{C}^T$.

III. Parameter estimation procedure

In support of our thesis that the motion of a non-maneuvering ship in open seas is better represented by an OU process on the target velocity rather than the NCV model, we analyzed a significant data set of real-world vessel trajectories in order to compare the SDE models described in the previous section. For this reason we need a procedure to establish the SDE parameters $\boldsymbol{\theta} = (\boldsymbol{\theta}_x, \boldsymbol{\theta}_y)$ of the processes; in the NCV case

$$\boldsymbol{\theta}_x = \sigma_x \quad \text{and} \quad \boldsymbol{\theta}_y = \sigma_y \tag{24}$$

while, under the OU assumption on the target velocity, we have

$$\boldsymbol{\theta}_x = (\sigma_x, \gamma_x, v_x) \quad \text{and} \quad \boldsymbol{\theta}_y = (\sigma_y, \gamma_y, v_y). \tag{25}$$

To avoid duplication, we will use $\boldsymbol{\theta}_{x,y}$, $\sigma_{x,y}$, $\gamma_{x,y}$ and $v_{x,y}$ to denote quantities that can equally refer to the x *or* y coordinate.

We shall now provide a description of the procedure adopted to estimate $\boldsymbol{\theta}$ for every given trajectory. Let us assume we have recorded a set of K trajectories of non-maneuvering vessels. In practice, the non-maneuverability assumption translates to the selection of piecewise linear vessel trajectories. Each trajectory is defined by a set of target states

$$\mathcal{S}_i = \{\boldsymbol{s}_i(t_{i,j})\}_{j=0}^{N_i}, \tag{26}$$

for $i = 1, \ldots, K$ at some time instants $t_{i,j-1}\,(< t_{i,j})$, for $j = 0, \ldots, N_i$. Assume we observe only the set of velocities denoted by

$$\mathcal{Z}_i = \{\dot{\boldsymbol{x}}_i(t_{i,j})\}_{j=0}^{N_i},$$

for $i = 1, \ldots, K$. Every trajectory i is characterized by $\boldsymbol{\theta}_i = (\boldsymbol{\theta}_{x,i}, \boldsymbol{\theta}_{y,i})$, which is estimated from the measurement set $\mathcal{Z}_i$ for both the NCV and OU models. Thanks to the Markovian and Gaussian properties of (6) and (8) [23], [28], the likelihood function of $\mathcal{Z}_i$ is explicitly given by [28]

$$\mathcal{L}_i(\boldsymbol{\theta}_i) = \prod_{j=1}^{N_i} \phi\left(\dot{\boldsymbol{x}}_i(t_{i,j})\,|\dot{\boldsymbol{x}}_i(t_{i,j-1}), \boldsymbol{\theta}_i\right), \tag{27}$$

where $\phi(\cdot)$ is a bivariate Gaussian distribution. The estimate is then provided by the ML estimator

$$\hat{\boldsymbol{\theta}}_i = \arg\max_{\boldsymbol{\theta}} \mathcal{L}_i(\boldsymbol{\theta}).$$

However, in order to simplify the estimation procedure from a computational perspective, we can use the marginal likelihood along x and y coordinates. This marginalization procedure is quite standard, especially from the Bayesian

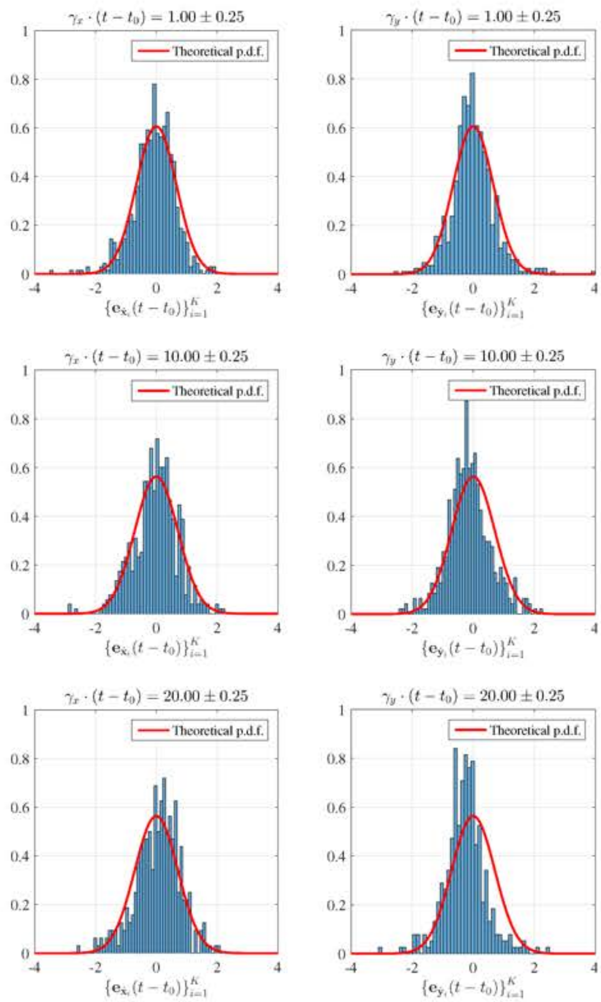

Fig. 2. Empirical and theoretical distributions of the normalized prediction error on the target velocity at two different time instants for the x (left) and y (right) components.

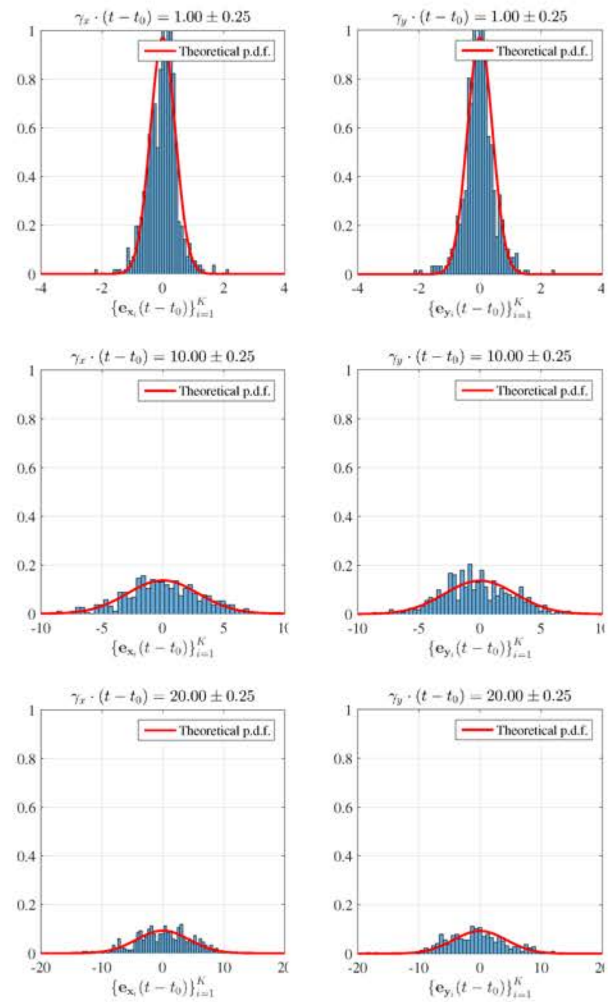

Fig. 3. Empirical and theoretical distributions of the normalized prediction error on the target position at two different time instants for the x (left) and y (right) components.

standpoint (assuming non-informative prior in our case) i.e. the other coordinate (y if we are estimating parameters along x and vice versa) is considered as a nuisance parameter. The marginal likelihoods are then given by:

$$\mathcal{L}_{x,i}\left(\boldsymbol{\theta}_{x,i}\right) = \prod_{j=1}^{N_i} \phi_{\dot{x}_i}\left(\dot{x}_i(t_{i,j})\,|\dot{x}_i(t_{i,j-1}), \boldsymbol{\theta}_{x,i}\right), \quad (28)$$

$$\mathcal{L}_{y,i}\left(\boldsymbol{\theta}_{y,i}\right) = \prod_{j=1}^{N_i} \phi_{\dot{y}_i}\left(\dot{y}_i(t_{i,j})\,|\dot{y}_i(t_{i,j-1}), \boldsymbol{\theta}_{y,i}\right). \quad (29)$$

where $\phi_{\dot{x}_i}(\cdot)$ and $\phi_{\dot{y}_i}(\cdot)$ are Gaussian distributions with mean and variance respectively given by the solution of the SDE (see also the discussion in Section II). Specifically, for the NCV we have

$$\mathrm{E}\left[\dot{x}_i(t_{i,j})|\,\dot{x}_i(t_{i,j-1})\right] = \dot{x}_i(t_{i,j-1}) \quad (30a)$$

$$\mathrm{E}\left[\,\dot{y}_i(t_{i,j})|\,\dot{y}_i(t_{i,j-1})\,\right] = \dot{y}_i(t_{i,j-1}) \quad (30b)$$

$$\mathrm{V}\left[\dot{x}_i(t_{i,j})|\,\dot{x}_i(t_{i,j-1})\right] = \sigma_x^2 \Delta_{i,j} \quad (30c)$$

$$\mathrm{V}\left[\,\dot{y}_i(t_{i,j})|\,\dot{y}_i(t_{i,j-1})\,\right] = \sigma_y^2 \Delta_{i,j} \quad (30d)$$

while for the OU we have

$$\mathrm{E}\left[\dot{x}_i(t_{i,j})|\,\dot{x}_i(t_{i,j-1})\right] = v_x + (\dot{x}_i(t_{i,j-1}) - v_x)e^{-\gamma_x \Delta_{i,j}} \quad (31a)$$

$$\mathrm{E}\left[\,\dot{y}_i(t_{i,j})|\,\dot{y}_i(t_{i,j-1})\,\right] = v_y + (\dot{y}_i(t_{i,j-1}) - v_y)e^{-\gamma_y \Delta_{i,j}} \quad (31b)$$

$$\mathrm{V}\left[\dot{x}_i(t_{i,j})|\,\dot{x}_i(t_{i,j-1})\right] = \frac{\sigma_x^2}{\gamma_x}\, g\left(\gamma_x \Delta_{i,j}\right) \quad (31c)$$

$$\mathrm{V}\left[\,\dot{y}_i(t_{i,j})|\,\dot{y}_i(t_{i,j-1})\,\right] = \frac{\sigma_y^2}{\gamma_y}\, g\left(\gamma_y \Delta_{i,j}\right) \quad (31d)$$

where $\mathrm{V}[\cdot]$ indicates the variance operator and $\Delta_{i,j} \overset{def}{=} t_{i,j} -$

$t_{i,j-1}$. The ML estimators along x and y for the i^{th} trajectory are given by

$$\hat{\boldsymbol{\theta}}_{x,i} = \arg\max_{\boldsymbol{\theta}_x} \mathcal{L}_{x,i}\left(\boldsymbol{\theta}_x\right),$$
$$\hat{\boldsymbol{\theta}}_{y,i} = \arg\max_{\boldsymbol{\theta}_y} \mathcal{L}_{y,i}\left(\boldsymbol{\theta}_y\right). \quad (32)$$

Further details about the implementation of the ML estimators are given in [14].

IV. Model validation criterion

Let us consider now the i^{th} trajectory, which is made up of a sequence of target states $\mathcal{S}_i$, as in (26), observed at the time instants $t_{i,j-1}$ $(< t_{i,j})$. Aiming to understand which one of the two models better represents the target motion, we take each data point of the trajectory and, using it as the initial target state, we perform the target state prediction at the time instants of the following observations. That is, given the initial state $\boldsymbol{s}_i(t_{i,j})$ for $j = 0, 1, ..., N_i$, we predict the sequence of target states at the time instants $t = t_{i,n}$ for $n = j+1, \ldots, N_i$:

$$\hat{\mathcal{S}}_i = \left\{ \left\{ \boldsymbol{s}_i(t_{i,n}|t_{i,j}) \right\}_{n=j+1}^{N_i} \right\}_{j=0}^{N_i},$$

where the estimate $\boldsymbol{s}_i(t_{i,n}|t_{i,j})$ is given by (10) for the NCV model, and by (15) for the OU model. The parameters $\boldsymbol{\theta}_i$ used in the prediction are estimated from the velocity samples themselves, as described in Section III.

We can now define the prediction error as a function of the prediction horizon $t > 0$:

$$\boldsymbol{e}_{\boldsymbol{s}_i}(t) \stackrel{def}{=} \left[\boldsymbol{e}_{\boldsymbol{x}_i}^T(t), \boldsymbol{e}_{\dot{\boldsymbol{x}}_i}^T(t)\right]^T$$
$$= \boldsymbol{s}_i(t+t_0) - \boldsymbol{s}_i(t+t_0|t_0), \quad (33)$$

which is a zero-mean random variable, as also shown in Fig. 2 and 3, where we report the empirical and theoretical distributions of the positional and velocity components of $\{\boldsymbol{e}_{\boldsymbol{s}_i}(t)\}_{i=1}^K$ at several time instants, for the positional and velocity components of the target state, respectively. The empirical distributions come from the real-world dataset, while the theoretical Probability Density Functions (PDFs) are zero-mean Gaussian distributions with variance defined by (18)–(21).

The dependency on the generic instant t_0 is not made explicit in the notation because we are interested only in its first and second moments, which are independent of t_0 because of the properties of the target process described in Section II. Therefore, we will consider hereafter that $t_0 = 0$, without affecting the analysis. Having predicted the target states at the time instants when the measurements are available, the prediction intervals for the i^{th} trajectory are

$$\mathcal{T}_i = \left\{ \left\{ t_{i,n} - t_{i,j} \right\}_{n=j+1}^{N_i} \right\}_{j=1}^{N_i},$$

meaning that the prediction error is sampled at the time instants $t \in \mathcal{T}_i$. The computed prediction error should correspond to the diagonal elements of (12) in the NCV case, and to (18)–(21) under the OU assumption on the target velocity. In order to verify the suitability of the models under investigation for the prediction uncertainty, we analyze the set of prediction errors $\{\boldsymbol{e}_{\boldsymbol{s}_i}(t)\}_{i=1}^K$ for both models versus the prediction horizon t.

The first hurdle is related to the fact that, as already discussed in Section III, each trajectory i is a realization of the stochastic process —on the target velocity— with a specific set of parameters $\boldsymbol{\theta}_i$. Also the data analysis and the model validation are affected by the inhomogeneity of the samples drawn from different trajectories, being these not directly comparable because of the different process parameters. The validation must, therefore, be carried out by separating the effect of the parameters from the time dependency in the diagonal entries of (12) and in (18)–(21). This is possible by normalizing the error in amplitude for the NCV and in both amplitude and time scale for the OU. Specifically, the error can be normalized as follows

$$\widetilde{\boldsymbol{e}}_{\boldsymbol{s}_i}(t) = \begin{cases} \boldsymbol{T}_i^{-1}\boldsymbol{e}_{\boldsymbol{s}_i}(t) & \text{if NCV,} \\ \boldsymbol{T}_i^{-1}\boldsymbol{e}_{\boldsymbol{s}_i}(t/\gamma_i) & \text{if OU,} \end{cases} \quad (34)$$

where

$$\boldsymbol{T}_i = \begin{cases} \text{diag}\left(\sigma_{x,i}, \quad \sigma_{y,i}, \quad \sigma_{x,i}, \quad \sigma_{y,i}\right) & \text{if NCV,} \\ \text{diag}\left(\frac{\sigma_{x,i}}{\gamma_x^{3/2}}, \quad \frac{\sigma_{y,i}}{\gamma_y^{3/2}}, \quad \frac{\sigma_{x,i}}{\gamma_x^{1/2}}, \quad \frac{\sigma_{y,i}}{\gamma_y^{1/2}}\right) & \text{if OU.} \end{cases} \quad (35)$$

In this way the second moment of $\widetilde{\boldsymbol{e}}_{\boldsymbol{s}_i}(t)$ is independent of i. Specifically, the error variance can be derived easily from the diagonal elements of (12) and from (18)–(21)

$$\boldsymbol{d}\left(\text{E}\left[\widetilde{\boldsymbol{e}}_{\boldsymbol{s}_i}(t)\widetilde{\boldsymbol{e}}_{\boldsymbol{s}_i}^T(t)\right]\right) = \boldsymbol{\eta}(t), \quad (36)$$

$$\boldsymbol{\eta}(t) \stackrel{def}{=} \begin{cases} \left[t^4/4, \quad t^4/4, \quad t^2, \quad t^2\right]^T & \text{if NCV,} \\ \left[f(t), \quad f(t), \quad g(t), \quad g(t)\right]^T & \text{if OU,} \end{cases} \quad (37)$$

where $\boldsymbol{d}(\cdot)$ is the vector of the diagonal elements, and the functions $f(t)$ and $g(t)$ are defined in (22)–(23).

At this point we can verify if the sample covariance of the normalized prediction error, provided by the data, fits the theoretical expectation $\boldsymbol{\eta}(t)$. This is possible by using

$$\boldsymbol{\eta}_K(t) \stackrel{def}{=} \frac{1}{K}\sum_{i=1}^{K} \boldsymbol{d}\left(\widetilde{\boldsymbol{e}}_{\boldsymbol{s}_i}(t)\widetilde{\boldsymbol{e}}_{\boldsymbol{s}_i}^T(t)\right) \stackrel{K\to\infty}{\to} \boldsymbol{\eta}(t), \quad (38)$$

where the convergence can be intended in mean square or in probability [29].

Roughly speaking, in our case, given a sufficiently large sample size K, then the sample variance of the normalized prediction error is close to the expected one $\boldsymbol{\eta}(t)$. In Section V we compare the empirical curve $\boldsymbol{\eta}_K(t)$ with the theoretical curve $\boldsymbol{\eta}(t)$ for both OU and NCV models.

V. Model validation using real-world vessel traffic data

In this section we provide evidence that the OU —for the velocity— and IOU —for the position— models fit better than the NCV to the uncertainty of long-term state predictions of non-maneuvering vessels.

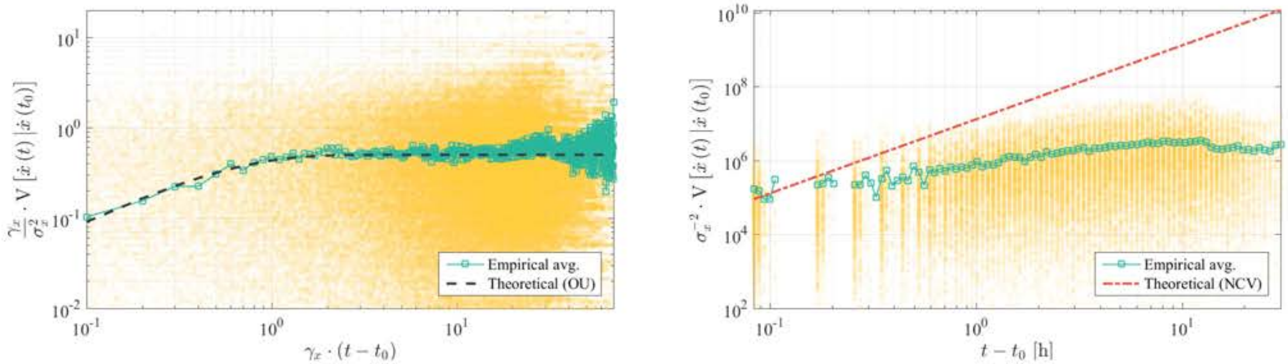

Fig. 4. Superimposition of all the realizations of the squared prediction error on the target velocity, for the OU (left) and NCV (right) models, together with the empirical variance and the theoretical model over the prediction time.

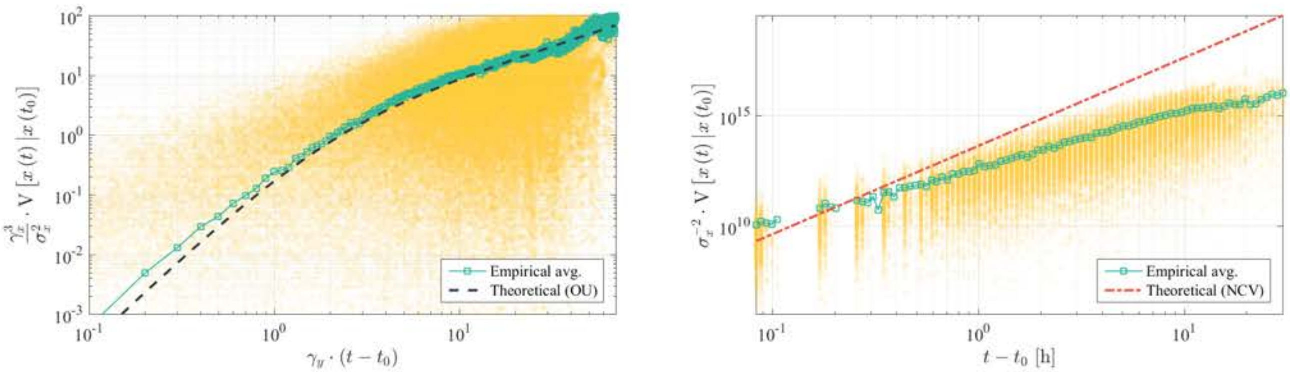

Fig. 5. Superimposition of all the realizations of the squared prediction error on the target position, for the OU (left) and NCV (right) models, together with the empirical variance and the theoretical model over the prediction time.

This evidence is based on the analysis of a significant record of the commercial maritime traffic in the Mediterranean Sea, collected by the NATO Science and Technology Organization (STO)-Centre for Maritime Research and Experimentation (CMRE). Specifically, the data set consists of AIS messages broadcast by commercial vessels in the Mediterranean Sea in two months of 2014 and collected by a network of receivers.

An initial step has to be accomplished before the actual analysis can start, because of the models described in Section II being valid under the assumption of a non-maneuvering vessel. This pre-processing phase consists of enforcing this assumption on the given real-world data set by breaking every observed trajectory into linear piecewise parts wherein the target has essentially no process noise.

This first step leaves us with a set of observed trajectories of non-maneuvering vessels. The prediction procedure is repeated for all the trajectories and for the different motion models, leading us to a collection of prediction errors relative to the target position and velocity as described in Section IV. The OU motion model for the velocity and its integrated version for the position, as described in Section II-A2, are characterized by three parameters for each coordinate: the noise level $\sigma_{x,y}$, the desired speed $\boldsymbol{v}$, and the reversion rate $\gamma_{x,y}$, which basically represents how quickly the target tends to restore its desired speed after a perturbation. The NCV motion model has instead just one parameter for each coordinate: the noise level $\sigma_{x,y}$.

It is apparent that these process parameters are important to the specific realization but, more importantly, they are not known a priori and therefore have to be estimated, see Section III. The estimation of the process parameters is not error-free but, on the contrary, introduces additional error. However, our analysis shows a good match between the real-data and the theoretical curves, meaning that the trajectories are sufficiently long to guarantee a parameter estimation with a negligible error.

Fig. 4 and 5 show the prediction error variance on the target velocity and position, respectively, over the prediction horizon. The plots on the left refer to the OU models, while those on the right to the NCV; for brevity, only the x component of the error is reported, being the y component analogous. In each figure, scatter plots illustrate the empirical data, i.e. the actual prediction error variance observed on the target velocity, whereas dashed lines represent the theoretical models. As discussed in Section IV, a normalization step, see (34), is necessary in order to compare the trends of the prediction uncertainty of all the trajectories in the data set. Therefore, the numerical values in OU and NCV plots do not show the actual variance of the prediction but rather represent the *normalized* variance. The OU the time axes have also been scaled according to the reversion rate of each trajectory, while this is not necessary for the NCV model.

From Fig. 4 and 5 it is also easy to recognize that, while the NCV models fit the empirical curve only in the short time prediction, the OU instead fits the whole evolution. It is worth mentioning that in the long time prediction the fundamental difference between the two model becomes clear: the NCV uncertainty diverges, as for a Brownian motion, while the OU reaches an asymptotic level provided by $g(t) \to 1/2$, see (37) and (23). The asymptotic unnormalized OU uncertainty is instead given by $\sigma_{x,y}^2/2\gamma_{x,y}$; basically it is proportional to the noise variance $\sigma_{x,y}^2$ and to the reversion rate $1/\gamma_{x,y}$. As already explained in Section II, the NCV model is equivalent to the OU for $\gamma_{x,y} \to 0$. This explains from another point of view why the NCV uncertainty diverges.

VI. Conclusion

We have studied the problem of issuing long-term predictions of future target states, with specific focus on the modeling of the related uncertainty. We have derived an optimal prediction procedure and investigated its variance over the prediction horizon.

Experimental results confirm that Ornstein-Uhlenbeck (OU) stochastic processes may be used to model the motion of non-maneuvering vessels while under way. Their major advantage over the more traditional NCV model is that the variance of the predicted position grows linearly with the prediction horizon, resulting a prediction uncertainty that is much more contained in larger time scales.

In the future, this model may be applied to relevant scenarios that might benefit from a more accurate modeling of the prediction uncertainty. For example, in the task of satellite image acquisition, the reduction of uncertainty in vessel location could enable higher resolution imagery over a smaller area, thus providing more accurate classification. Future investigations are needed to study on-line procedures for estimating and updating the OU parameters while the data are observed.

Acknowledgement

L. M. Millefiori, P. Braca and K. Bryan are supported by the NATO Supreme Allied Command Transformation (SACT) under project SAC000608 – Data Knowledge Operational Effectiveness.

References

[1] B. Ristic, B. La Scala, M. Morelande, and N. Gordon, "Statistical analysis of motion patterns in AIS data: Anomaly detection and motion prediction," in *Proc. of the* 11^{th} *Intern. Conf. on Inform. Fusion (FUSION)*, Florence, Italy, 2008.

[2] M. Vespe, I. Visentini, K. Bryan, and P. Braca, "Unsupervised learning of maritime traffic patterns for anomaly detection," in *Data Fusion Target Tracking Conference (DF TT 2012): Algorithms Applications, 9th IET*, May 2012.

[3] G. Pallotta, M. Vespe, and K. Bryan, "Vessel pattern knowledge discovery from AIS data: A framework for anomaly detection and route prediction," *Entropy*, vol. 15, no. 6, 2013.

[4] H. Wang, T. Kirubarajan, and Y. Bar-Shalom, "Precision large scale air traffic surveillance using IMM/assignment estimators," *IEEE Trans. Aerosp. Electron. Syst.*, vol. 35, no. 1, pp. 255–266, Jan. 1999.

[5] X. Rong Li and V. Jilkov, "Survey of maneuvering target tracking. part I. Dynamic models," *IEEE Trans. Aerosp. Electron. Syst.*, vol. 39, no. 4, pp. 1333–1364, Oct. 2003.

[6] X. R. Li and V. Jilkov, "Survey of maneuvering target tracking. Part II. Motion models of ballistic and space targets," *IEEE Trans. Aerosp. Electron. Syst.*, vol. 46, no. 1, pp. 96–119, Jan. 2010.

[7] *Safety of Life at Sea (SOLAS) Convention*. Chapter V, Regulation 19.

[8] C. of the European Communities, "Document com(2008) 310 final - 2005/0239 cod, brussels 11- 06-2008."

[9] Y. Bar-Shalom, P. Willett, and X. Tian, *Tracking and Data Fusion: A Handbook of Algorithms*. Storrs, CT: YBS Publishing, Apr. 2011.

[10] S. Maresca, P. Braca, J. Horstmann, and R. Grasso, "Maritime surveillance using multiple high-frequency surface-wave radars," *IEEE Trans. Geosci. Remote Sens.*, vol. 52, no. 8, pp. 5056–5071, Aug. 2014.

[11] P. Braca, P. Willett, K. LePage, S. Marano, and V. Matta, "Bayesian tracking in underwater wireless sensor networks with port-starboard ambiguity," *IEEE Trans. Signal Process.*, vol. 62, no. 7, pp. 1864–1878, 2014.

[12] G. Pallotta, S. Horn, P. Braca, and K. Bryan, "Context-enhanced vessel prediction based on Ornstein-Uhlenbeck processes using historical AIS traffic patterns: Real-world experimental results," in *Information Fusion (FUSION), 2014 17th International Conference on*, July 2014, pp. 1–7.

[13] L. M. Millefiori, G. Pallotta, S. Horn, P. Braca, and K. Bryan, "Validation of the Ornstein-Uhlenbeck route propagation model in the mediterranean sea," in *Proc. of the OCEANS'15 MTS/IEEE Conference*, May 2015, pp. 1–7.

[14] L. M. Millefiori, P. Braca, K. Bryan, and P. Willett, "Modeling vessel kinematics using a stochastic mean-reverting process for long-term prediction," *IEEE Trans. Aerosp. Electron. Syst.*, submitted for publication.

[15] L. D. Stone, C. A. Barlow, and T. L. Corwin, *Bayesian multiple target tracking*. Artech House, 1999.

[16] S. Coraluppi and C. Carthel, "Stability and stationarity in target kinematic modeling," in *IEEE Aerospace Conference,*, March 2012, pp. 1–8.

[17] ——, "A hierarchical MHT approach to ESM-radar fusion," in *Information Fusion (FUSION), 2012 15th International Conference on*, July 2012, pp. 677–683.

[18] ——, "Stochastic data association in multi-target filtering," in *Proc. SPIE*, vol. 8393, 2012, pp. 83 930Q–83 930Q–7.

[19] ——, "Advances in multi-target filtering of evasive targets," in *Aerospace Conference, 2015 IEEE*, March 2015, pp. 1–8.

[20] G. Vivone, P. Braca, and J. Horstmann, "Knowledge-based multi-target tracking via UKF-JPDA variable structure IMM estimator in HF surface wave radar systems," *IEEE Trans. Geosci. Remote Sens.*, 2015.

[21] G. Capraro, A. Farina, H. Griffiths, and M. Wicks, "Knowledge-based radar signal and data processing: a tutorial review," *IEEE Signal Process. Mag.*, vol. 23, no. 1, pp. 18–29, Jan. 2006.

[22] A. Benavoli, L. Chisci, A. Farina, L. Timmoneri, and G. Zappa, "Knowledge-based system for multi-target tracking in a littoral environment," *IEEE Trans. Aerosp. Electron. Syst.*, vol. 42, no. 3, pp. 1100–1119, July 2006.

[23] B. Øksendal, *Stochastic differential equations*. Springer, 2003.

[24] P. Langevin, "Sur la thorie du mouvement brownien," *C. R. Acad. Sci. (Paris)*, pp. 530–533, 1908.

[25] D. Gillespie, "Exact numerical simulation of the Ornstein-Uhlenbeck process and its integral," *Phys. Rev. E*, vol. 54, no. 2, pp. 2084–2091, 1996.

[26] G. E. Uhlenbeck and L. S. Ornstein, "On the theory of Brownian motion," *Phys. Rev.*, vol. 36, pp. 823–841, 1930.

[27] O. E. Barndorff-Nielsen and N. Shephard, "Integrated OU processes and non-Gaussian OU-based stochastic volatility models," *Scand. J. Statist.*, vol. 30, no. 2, pp. 277–295, Jun. 2003.

[28] L. Valdivieso, W. Schoutens, and F. Tuerlinckx, "Maximum likelihood estimation in processes of Ornstein-Uhlenbeck type," *Statistical Inference for Stochastic Processes*, vol. 12, no. 1, pp. 1–19, 2009.

[29] E. Lehmann, *Elements of Large Sample Theory*. Springer, 2004.

Document Data Sheet

Security Classification		Project No.
Document Serial No. CMRE-PR-2019-087	Date of Issue June 2019	Total Pages 8 pp.

Author(s)

Leonardo M. Millefiori, Paolo Braca, Karna Bryan, Peter Willett

Title

Long-term vessel kinematics prediction exploiting mean-reverting processes

Abstract

Long-term target state estimation of non-manoeuvring targets, such as vessels under way in open sea, is crucial for maritime security. The dynamics of non-manoeuvring targets is traditionally modelled with a white noise random process on the velocity, which is assumed to be nearly-constant. We show that this model might be an implausible hypothesis for a significant portion of maritime ship traffic, as vessels under way tend to adjust their speed continuously around a desired value. Additionally, vessels will naturally seek to optimize fuel consumption. We developed a method to predict long-term target states based on mean-reverting stochastic processes. Specifically, we use the Ornstein-Uhlenbeck (OU) process, leading to a revised target state equation and to a completely different time scaling law for the related uncertainty, which in the long term is shown to be orders of magnitude lower than nearly-constant velocity assumption. The proper modelling provides some improvement in accuracy; but the real benefit is improved track-stitching when there are lengthy gaps in observability. In support of the proposed model, we propose a large-scale analysis of a significant portion of the real-world maritime traffic in the Mediterranean Sea.

Keywords

Mathematical model, predictive models, target tracking, gold, uncertainty, marine vehicles, accidents

Issuing Organization

NATO Science and Technology Organization
Centre for Maritime Research and Experimentation

Viale San Bartolomeo 400, 19126 La Spezia, Italy

[From N. America:
STO CMRE
Unit 31318, Box 19, APO AE 09613-1318]

Tel: +39 0187 527 361
Fax:+39 0187 527 700

E-mail: library@cmre.nato.int